Electronic Supplementary Information (ESI)

High Performance Solution-processable Tetrathienoacene (TTAR) based Small Molecules for Organic Field Effect Transistors (OFETs)

Sureshraju Vegiraju,‡[a] Deng-Yi Huang,‡[b] Pragya Priyanka,[a] Yo-Shan Li,[a] Xian-Lun Luo,[b] Shao-Huan Hong,[b] Jen-Shyang Ni,[c] Shih-Huang Tung,[d] Chien-Lung Wang,[e] Wei-Chieh Lien,[a] Shueh Lin Yau,[a] Cheng-Liang Liu*[b] and Ming-Chou Chen*[a]

[a]*Department of Chemistry, National Central University, Taoyuan, 32001 Taiwan. E-mail: mcchen@ncu.edu.tw*

[b]*Department of Chemical and Materials Engineering, National Central University, Taoyuan, 32001 Taiwan. E-mail: clliu@ncu.edu.tw*

[c]*Institute of Chemistry, Academia Sinica, Taipei, 11529 Taiwan.*

[d]*Institute of Polymer Science and Engineering, National Taiwan University, Taipei, 10617 Taiwan.*

[e]*Department of Applied Chemistry, National Chiao Tung University, Hsinchu, 30010 Taiwan.*

‡ These authors contributed equally.

Experimental Section

Materials

All chemicals and solvents were of reagent or anhydrous grade and were obtained from Aldrich, Alfa and TCI Chemical Co. Solvents for reactions (toluene and THF) were distilled under nitrogen from sodium/benzophenone ketyl, and halogenated solvents were distilled from CaH_2. Dibromotetrathienoacene (4),[1] tributyl(dithieno[3,2-b:2',3'-d]thiophen-2-yl)stannane (5),[2] tributyl(thieno[3,2-b]thiophen-2-yl)stannane (6),[3] tributyl(thiophen-2-yl)stannane (7)[4] were prepared according to the procedures described in the literature. The silane agent for the self-assembly monolayer (SAM) treatment, (2-phenylethyl)trichlorosilane (PETS) or octadecyltrimethoxysilane (ODTS), was supplied from Gelest, Inc.

General characterization methods

^1H and ^{13}C NMR were recorded using a Bruker 500 or 300 instrument for all materials, with reference to solvent signals. Elemental analyses were performed on a Heraeus CHN-O-Rapid elemental analyzer. Mass spectrometric data were obtained with a JMS-700 HRMS instrument. Differential scanning calorimetry (DSC) was carried out under nitrogen on a Mettler DSC 822 instrument (scanning rate of 10 °C min^{-1}). Thermogravimetric analysis (TGA) was carried out using a Perkin Elmer TGA-7 thermal analysis system, using dry nitrogen as a carrier gas at a flow rate of 10 mL min^{-1} (heating rate of 10 °C min^{-1}), and reported decomposition temperatures represent the temperature observed at 5 % mass loss. UV-Vis absorption was carried out in the indicated solvents at room temperature with a JASCO V-530 spectrometer. Differential pulse voltammetry (DPV) experiments were performed with a conventional three-electrode configuration (a platinum disk working electrode, an auxiliary platinum wire electrode, and a non-aqueous Ag reference electrode, with a supporting electrolyte of 0.1 M tetrabutylammoniumhexafluorophosphate ($TBAPF_6$) in the specified dry solvent) using a

CHI621C Electrochemical Analyzer (CH Instruments). All electrochemical potentials were referenced to an Fc^+/Fc internal standard (at 0.6 V). The surface morphology of solution-sheared organic semiconductor thin film was observed by polarized optical microscopy (POM; Leica 2700M) and atomic force microscopy (tapping mode AFM; Seiko SPA400). Grazing incident X-ray diffraction (GIXRD) was collected at beamline B13A1 and B17A1 at the National Synchrotron Radiation Research Center (NSRRC, Taiwan).

General procedures for the target compounds (1-3)

Under anhydrous conditions, $Pd(PPh_3)_4$ (0.05 equiv.) was added to a solution of dibromotetrathienoacene (**4**, 1 equiv.) and mono-stannylated compounds (**5-7**; 2.3 equiv.) in dry toluene. The resulting mixture was refluxed overnight under nitrogen. After filtration through silica and removal of the solvent, the desired product was collected by filtration, washed with hexanes, and recrystallized from toluene, thus producing highly pure target molecules for device fabrication.

Compound DT-TTAR (1)

The title compound was obtained as a pale yellow solid (yield = 71%). Mp: 120 °C. ^{1}H NMR (300 MHz, $CDCl_3$): δ 7.34 (d, J = 4.8 Hz, 2 H), 7.19 (d, J = 3.6 Hz, 2 H), 7.11 (t, J = 4.4 Hz, 2 H), 2.91 (t, J = 8.1 Hz, 4 H), 1.78 (m, 4 H), 1.26 (br, 48 H), 0.88 (t, J = 6.9 Hz, 6 H). ^{13}C NMR (125 MHz, $CDCl_3$): δ 142.48, 136.32, 133.02, 132.06, 131.16, 129.37, 127.53, 126.48, 125.98, 31.94, 29.67, 29.54, 29.36, 29.07, 28.78, 22.68, 14.05. HRMS (*m/z*, FAB+) calcd for $C_{48}H_{68}S_6$: 836.3645, found 836.3655.

Compound DTT-TTAR (2)

The title compound was obtained as a yellow solid (yield = 81%). Mp: 161 °C. ^{1}H NMR (300 MHz, $CDCl_3$): δ 7.41 (d, J = 5.5 Hz, 2 H), 7.36 (s, 2 H), 7.27 (d, J = 7.0 Hz, 2 H), 2.97 (t, J =

8.0 Hz, 4 H), 1.82 (m, 4 H), 1.27 (br, 48 H), 0.88 (t, J = 7.0 Hz, 6 H). ^{13}C NMR (75 MHz, $CDCl_3$): δ 142.66, 139.65, 139.56, 138.02, 133.56, 132.25, 131.44, 129.78, 127.40, 119.42, 118.68, 31.95, 29.68, 29.55, 29.36, 29.18, 28.86, 22.68, 14.05. HRMS (*m/z*, FAB+) was calcd. for $C_{52}H_{68}S_8$ 948.3087, and 948.3096 was found.

Compound DT-TTAR (3)

The title compound was obtained as an orange solid (yield = 85%). Mp: 168 °C. ^{1}H NMR (300 MHz, $CDCl_3$): δ 7.40 (d, J = 5.0 Hz, 2 H), 7.38 (s, 2 H), 7.32 (d, J = 5.5 Hz, 2 H) ,2.99 (t, J = 8.5 Hz, 4 H), 1.84 (m, 4 H), 1.26 (br, 48 H), 0.88 (t, J = 7.0 Hz, 6 H). This material was insufficiently soluble to obtain a ^{13}CNMR spectrum (as shown in Fig. S9, ^{13}C NMR ($CDCl_3$) of **DDTT-TTAR)**. HRMS (*m/z*, FAB+) was calcd. for $C_{56}H_{68}S_{10}$ 1060.2528, and 1060.2526 was found.

OFET fabrication and measurement

Bare Si/SiO_2 wafer pieces were used as a substrate, where highly n-doped Si and 300 nm-thick SiO_2 served as the bottom gate electrode and dielectric layer, respectively. The clean substrate was treated by PETS (immersion in a solution of 1 μl ml^{-1} in toluene, kept at 50 ^{o}C for 90 min) to form SAM. The organic active layer was deposited on the OTS-treated substrate by solution-shearing in ambient atmosphere from chlorobenzene or 1,2,3,4-tetrahydronaphthalene (tetralin) solution with a concentration of 2~3 mg ml^{-1}. The shearing rate was controlled at 5~30 μm s^{-1} and the substrate was heated at 60~150 ^{o}C. The resulting film was then annealed at 50 ^{o}C under a vacuum for 30 min to remove the solvent residue. Au source/drain electrodes with a thickness of 80 nm were deposited on top of the organic semiconductor layer through a shadow mask with length (L)/width (W) of 25/1000 μm. The OFET measurements were carried out at room temperature inside a N_2-filled glove box with a Keithley 4200-SCS semiconductor

parameter analyzer. Field effect mobility (μ) and threshold voltage (V_{th}) were extracted in the saturation region using the following relationship:

$$I_d = \frac{W}{2L} C\mu (V_g - V_{th})^2 \quad (1)$$

where I_d is the drain current, V_g is the drain voltage and C is the oxide capacitance. The μ and V_{th} can be estimated from the slope and intercept of the linear section of the plot of $I_d^{1/2}$ vs V_g, respectively. The average TFT characteristics with standard deviations were obtained from more than ten devices originating from 3-4 semiconductor depositions.

DFT calculation

All theoretical computations were performed with Gaussian 03 software using the B3LYP/6-31G* level.

References

1. N. Zhou, S. Vegiraju, X. Yu, E. F. Manley, M. R. Butler, M. J. Leonardi, P. Guo, W. Zhao, Y. Hu, K. Prabakaran, R. P. H. Chang, M. A. Ratner, L. X. Chen, A. Facchetti, M.-C. Chen and T. J. Marks, *J. Mater. Chem. C.*, 2015, **3**, 8932-8941.
2. M.-C. Chen, S. Vegiraju, C.-M. Huang, P.-Y. Huang, K. Prabakaran, S. L. Yau, W.-C. Chen, W.-T. Peng, I. Chao, C. Kim and Y.-T. Tao, *J. Mater. Chem. C.*, 2014, **2**, 8892-8902.
3. S. Vegiraju, Y.-Y. Liu, K. Prabakaran, J.-S. Ni, Y. Ezhumalai, H.-C. Yu, S. L. Yau, J. T. Lin, M.-C. Chen and T.-C. Lin, *RSC. Adv.*, 2015, **5**, 54003-54010.
4. P. Priyanka, S. Vegiraju, J.-Y. Lin, J.-S. Ni, H.-Y. Huang, R. Dwi Agustin, S. L. Yau, T.-C. Lin and M.-C. Chen, *Dyes. Pigm.*, 2016, **133**, 65-72.

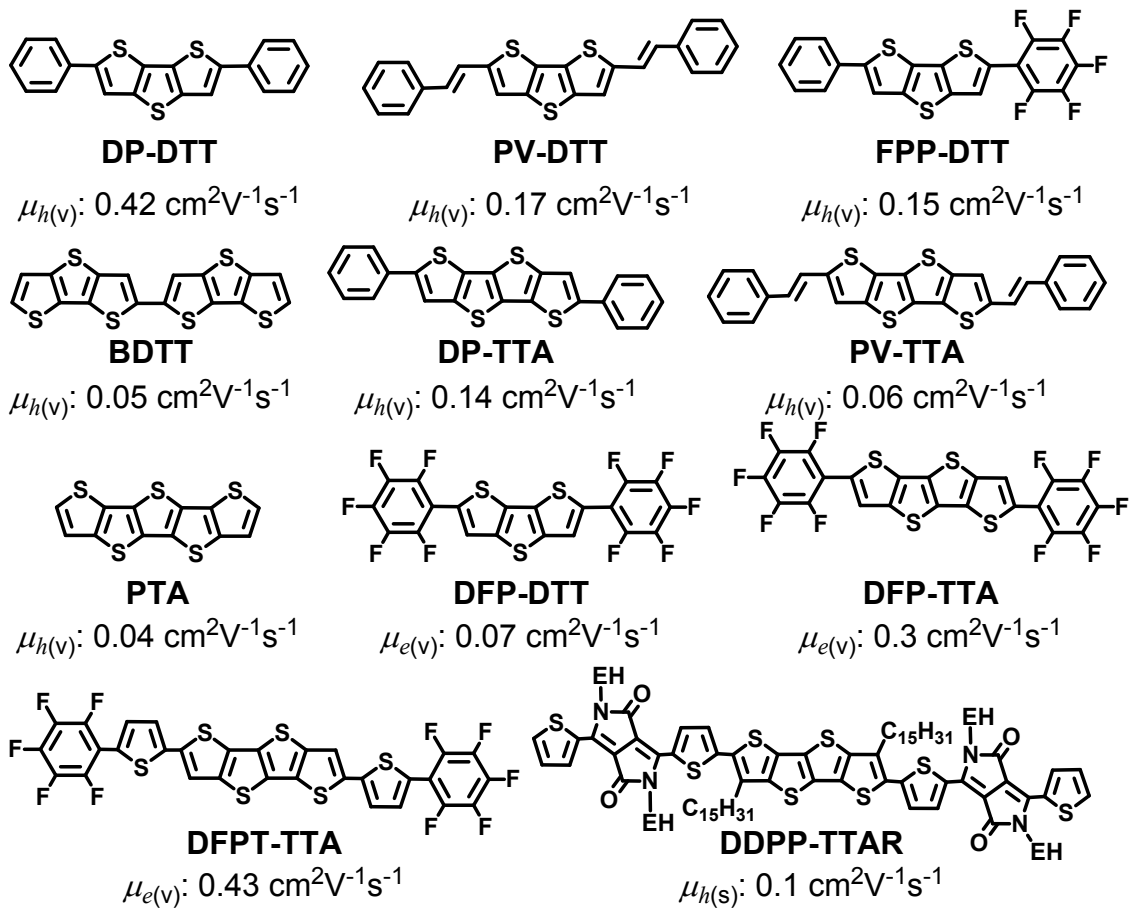

Fig. S1 Examples of fused thiophene-based small organic semiconductors for p and n-channel OFETs. ((v) denotes vacuum deposition and (s) a solution process)).

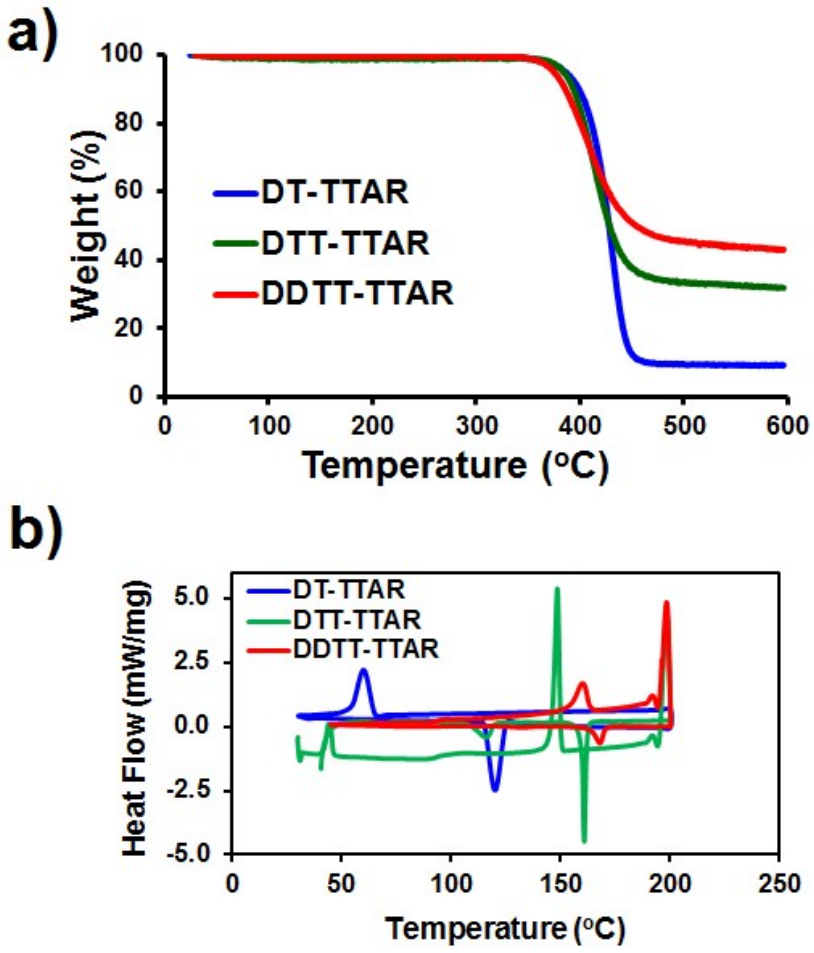

Fig. S2 (a) TGA and (b) DSC curves of **DT-TTAR**, **DTT-TTAR**, and **DDTT-TTAR** measured in the N_2 atmosphere.

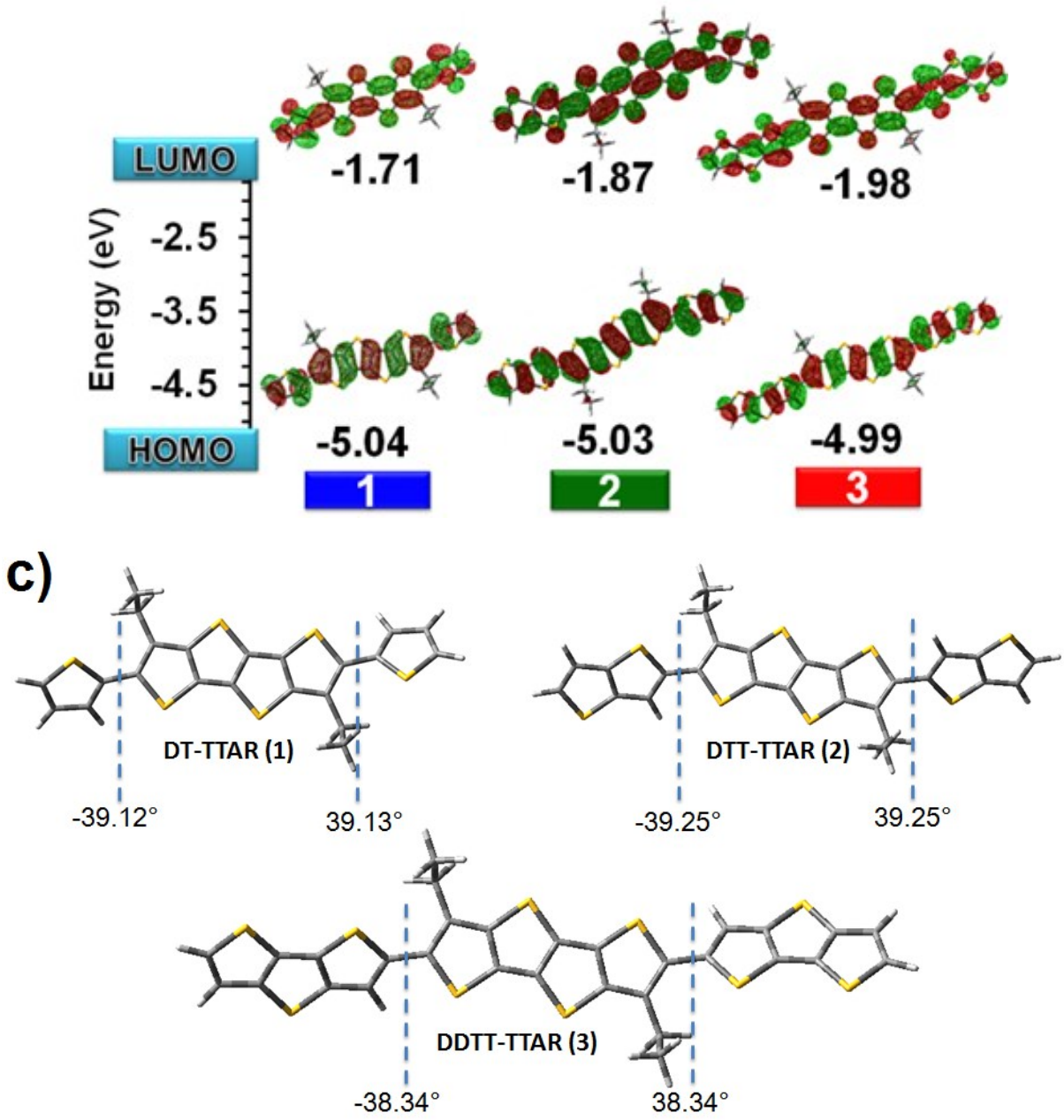

Fig. S3 (a) DFT-derived molecular orbital contours of three **TTAR**s and their calculated HOMO and LUMO energy levels. (b) Dihedral angles of three **TTAR**s from DFT calculations.

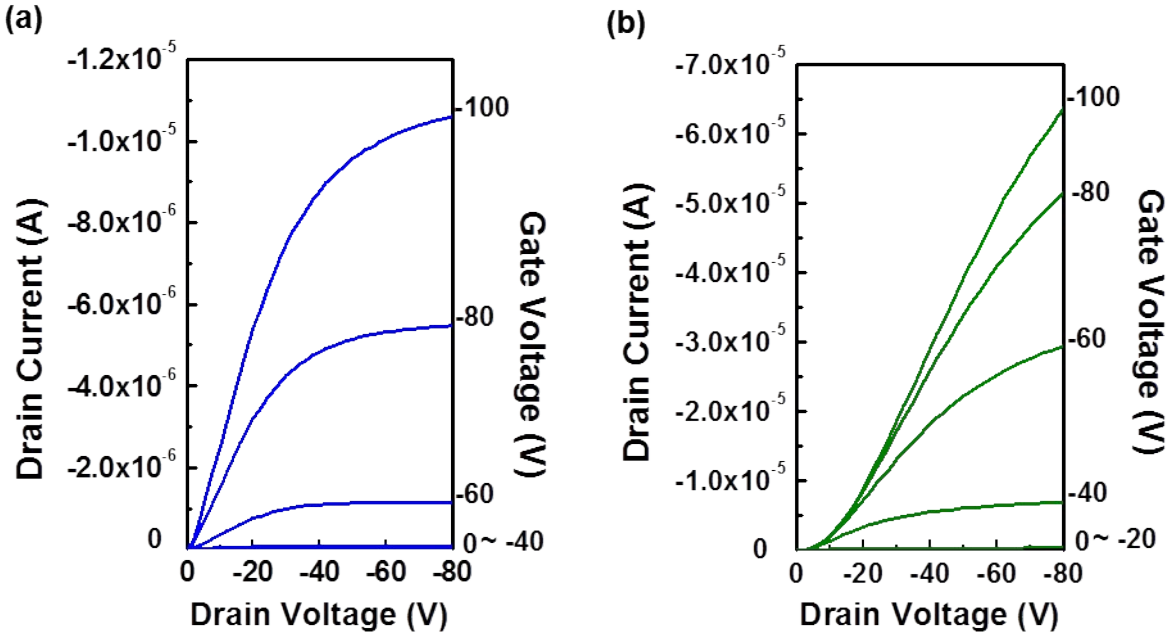

Fig. S4 Output characteristics of (a) **DT-TTAR** and (b) **DTT-TTAR** OFETs.

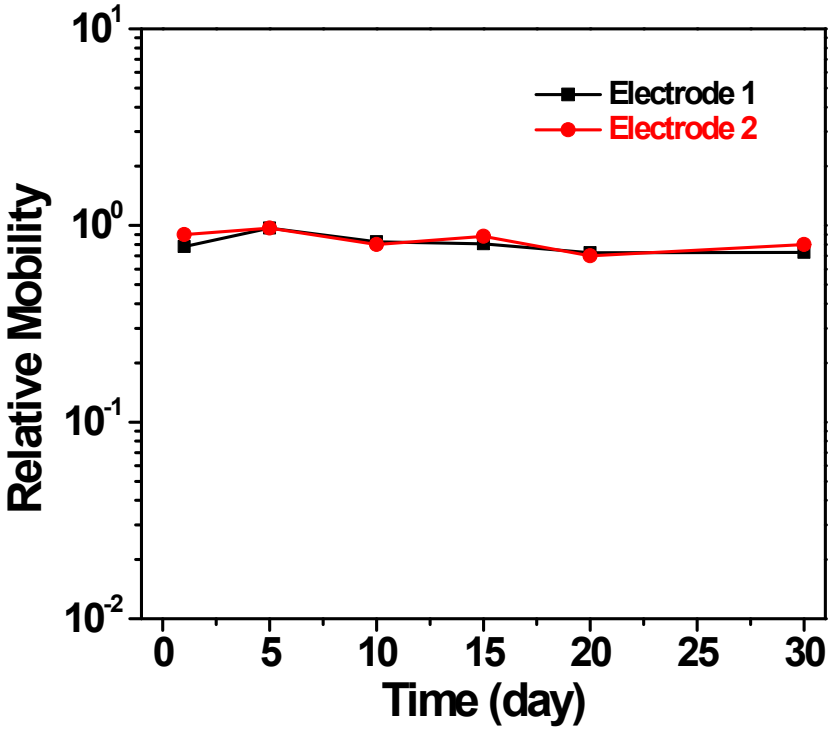

Fig. S5 Long term environmental stability of **DDTT-TTAR** OFETs in different batches, stored in ambient atmosphere.

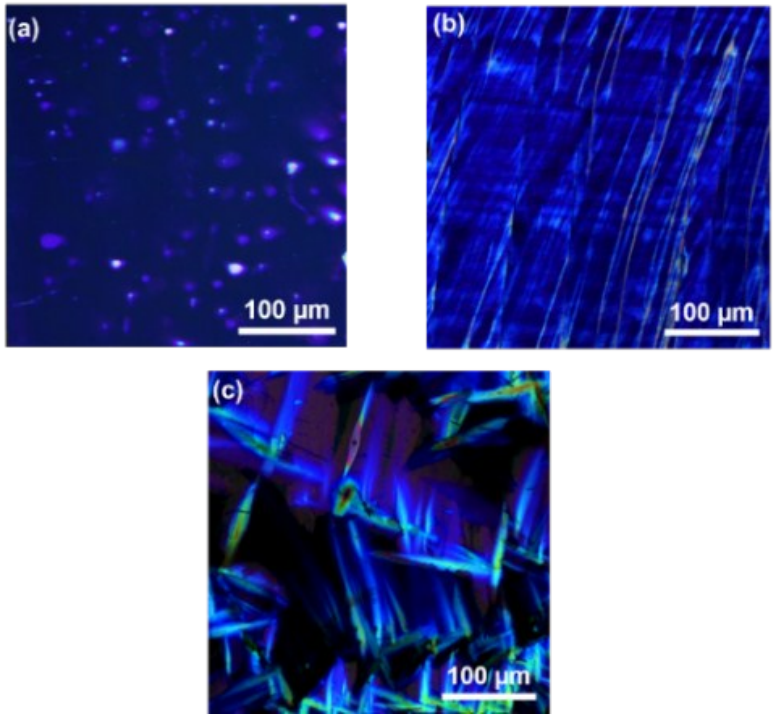

Fig. S6 POM image of solution-sheared (a) **DT-TTAR**, (b) **DTT-TTAR** and (c) **DDTT-TTAR** thin film.

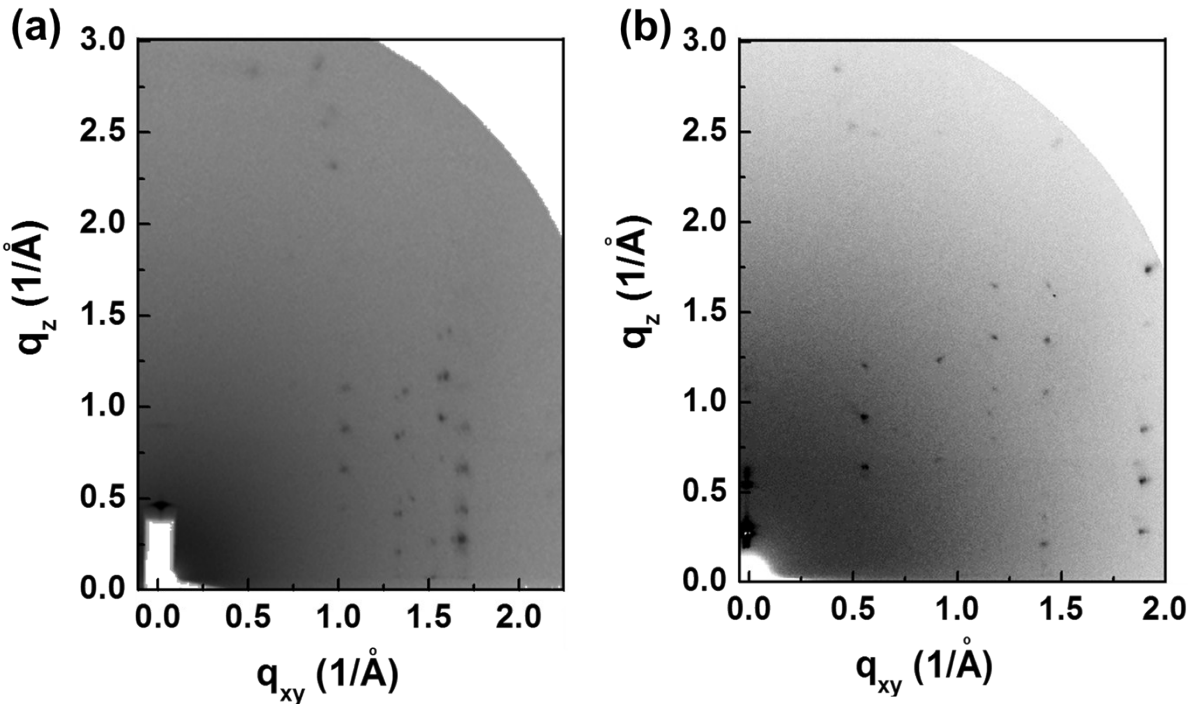

Fig. S7 GIXRD diffraction pattern image of solution-sheared (a) **DT-TTAR** and (b) **DTT-TTAR** thin film.

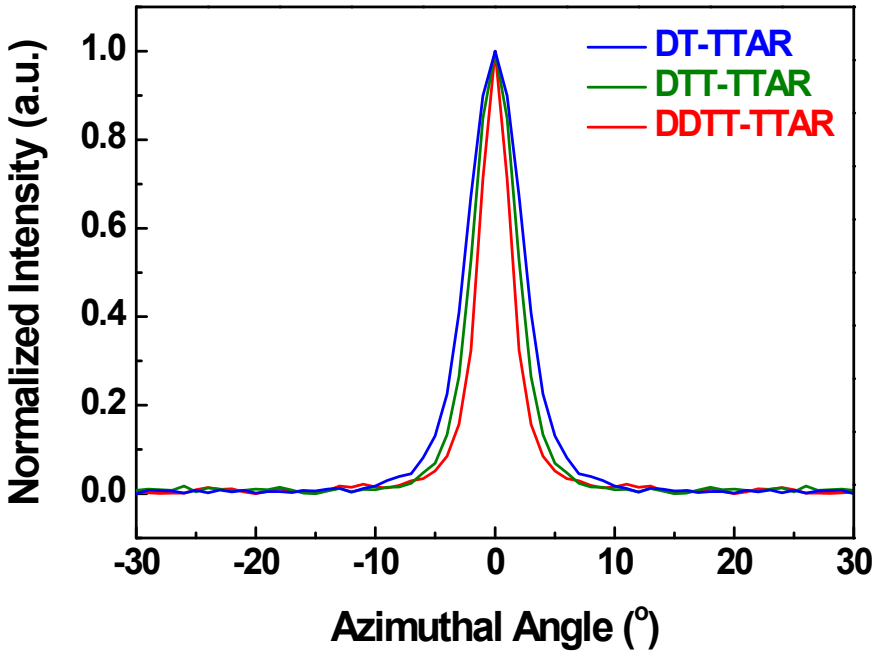

Fig. S8 X-ray diffraction (002) azimuthal scan profiles.

Fig. S9 ^{1}H NMR spectrum of **DT-TTAR**, **DTT-TTAR**, and **DDTT-TTAR**.

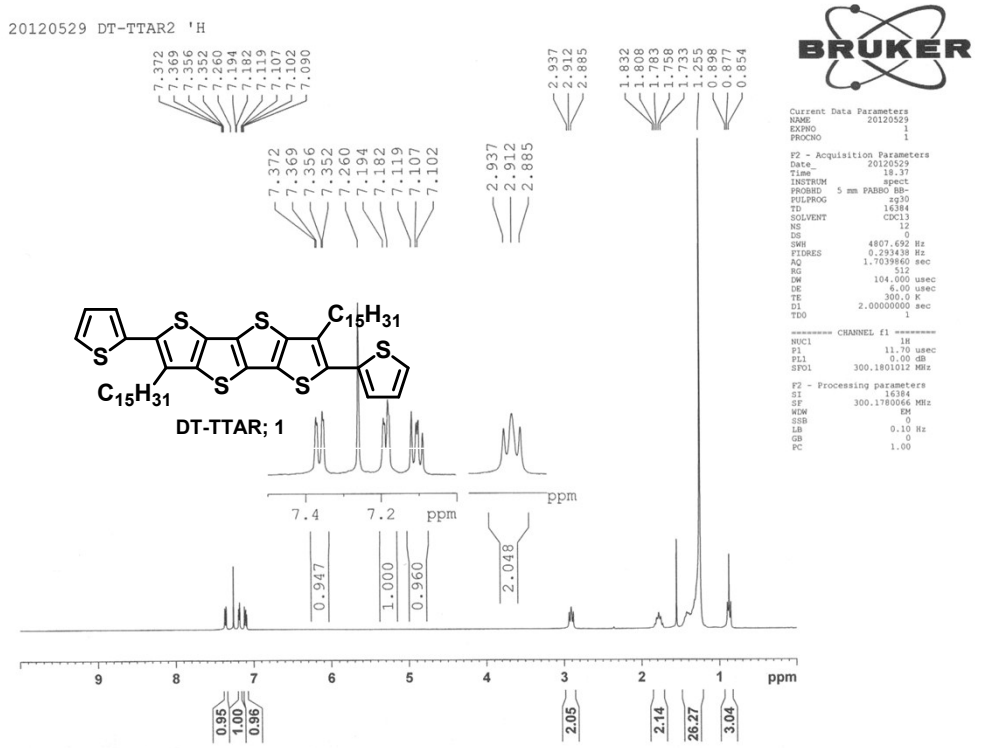

^{1}H NMR ($CDCl_3$) of DT-TTAR (1)

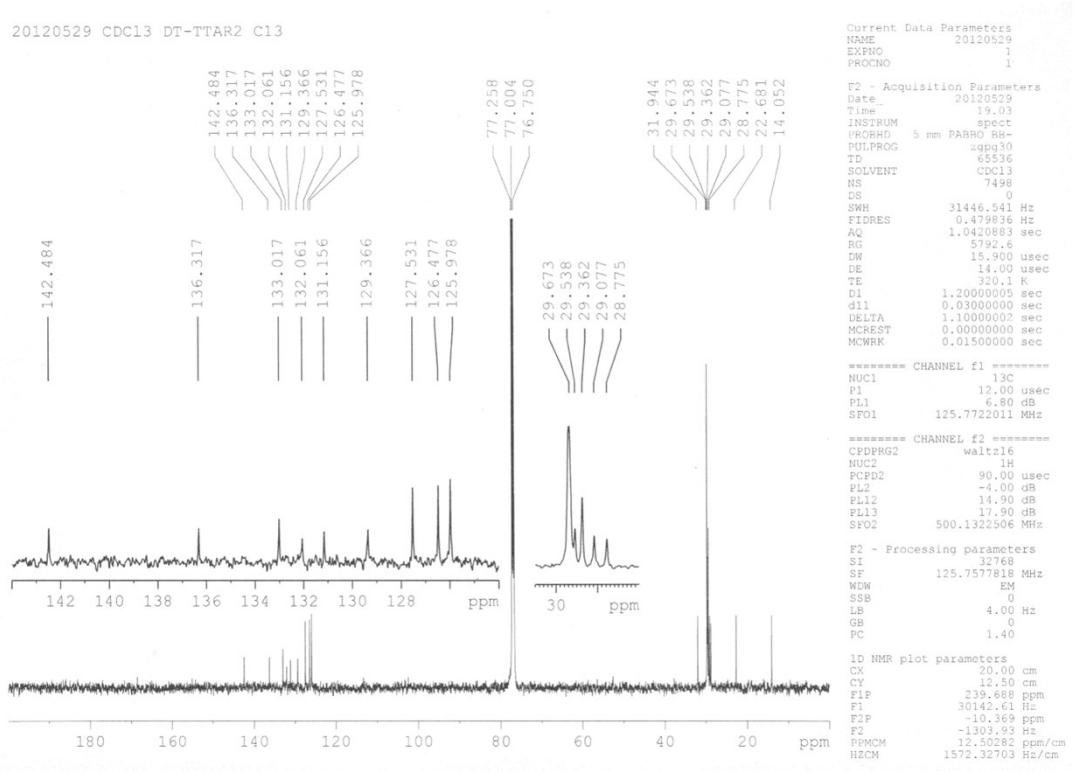

^{13}C NMR ($CDCl_3$) of DT-TTAR (1)

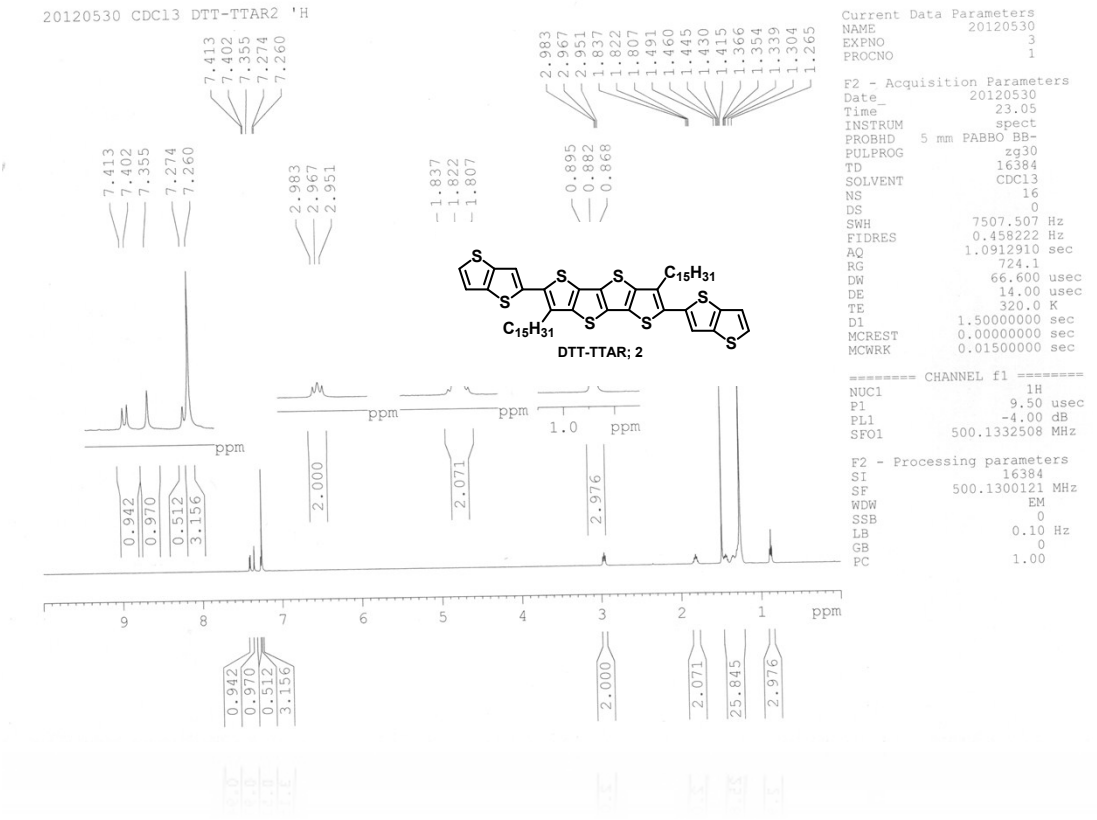

^{1}H NMR ($CDCl_3$) of DTT-TTAR (2)

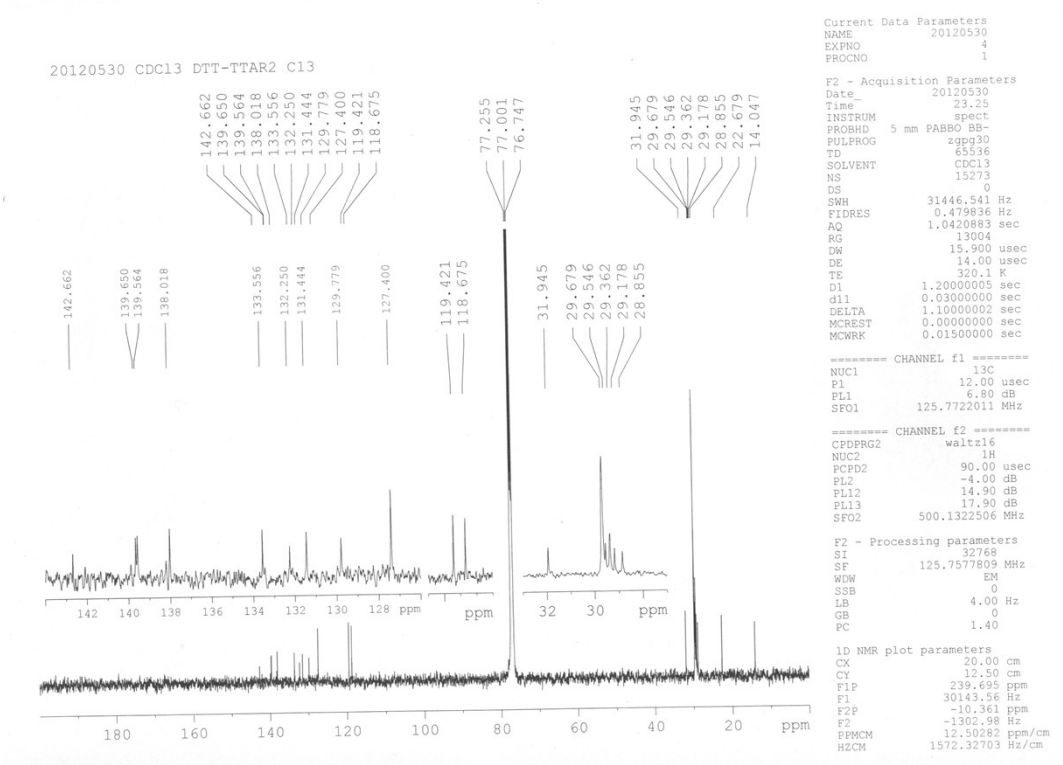

^{13}C NMR ($CDCl_3$) of DTT-TTAR (2)

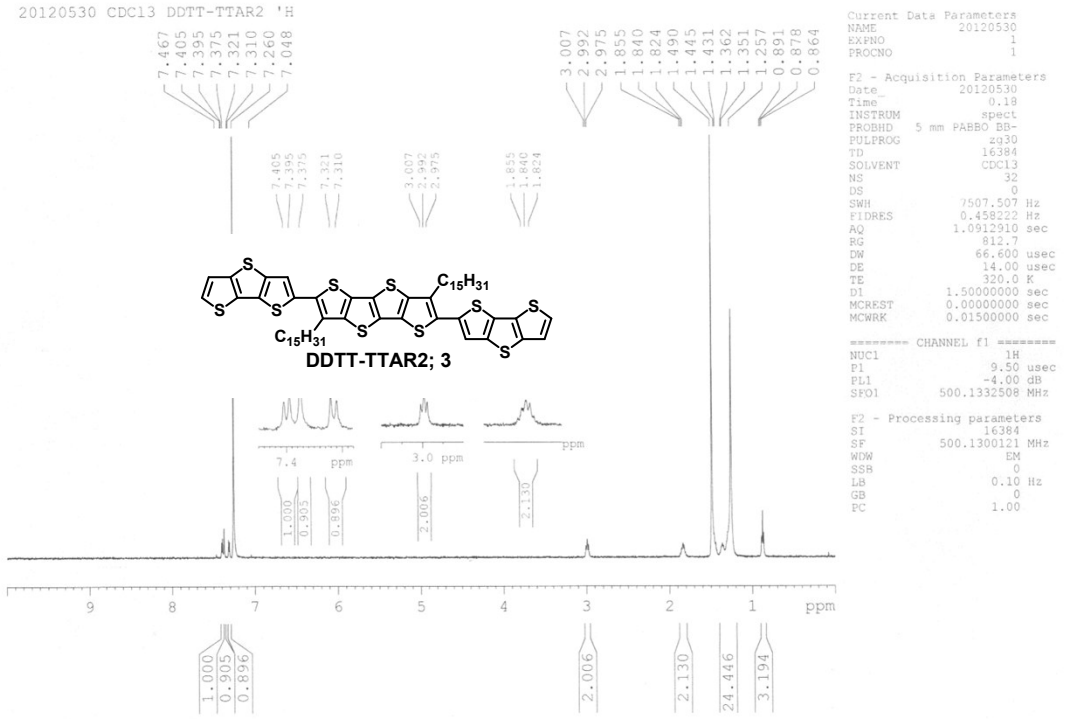

^{1}H NMR ($CDCl_3$) of DDTT-TTAR (3)

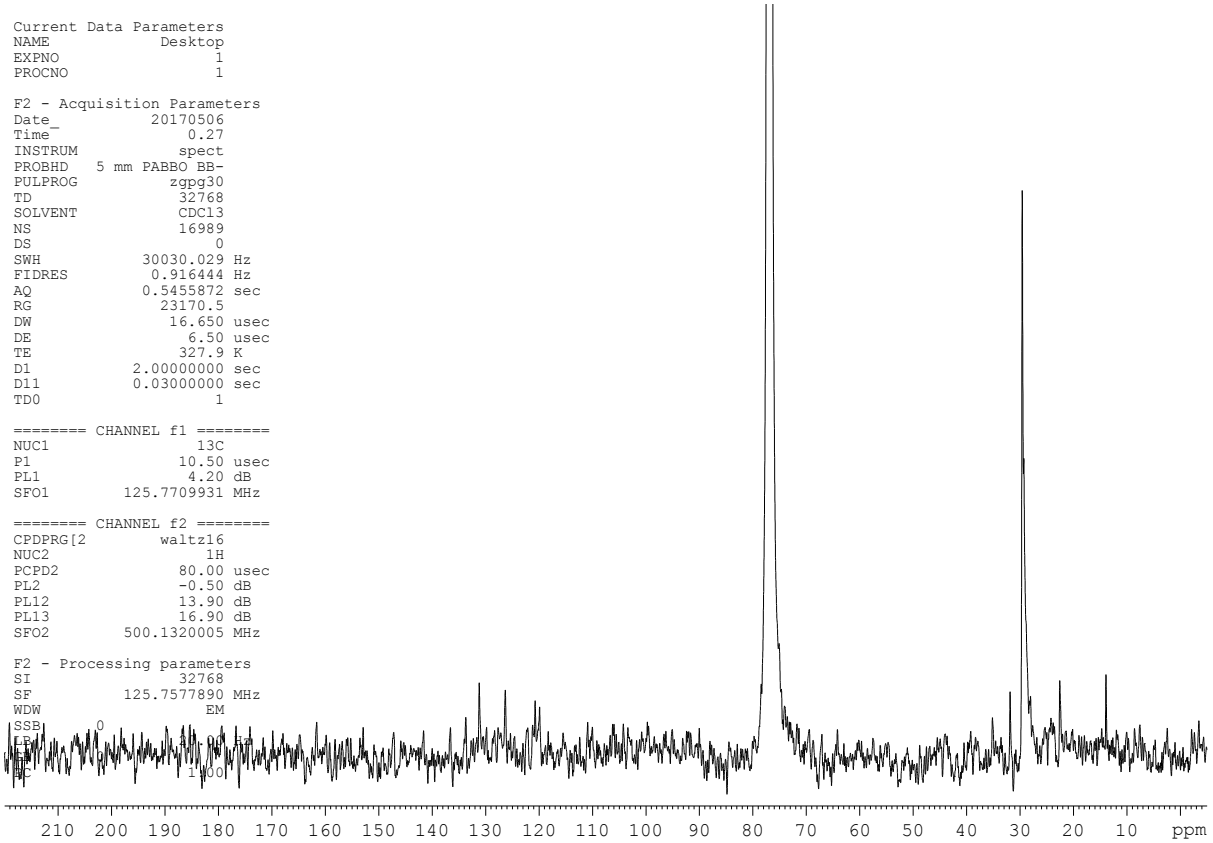

^{13}C NMR ($CDCl_3$) of DDTT-TTAR (3) (Poor solubility)